



SANDIA REPORT

SAND2001-8184
Unlimited Release
Printed June 2001

The Tritium Performance of Alloy 22-13-5

S. L. Robinson

Prepared by
Sandia National Laboratories
Albuquerque, New Mexico 87185 and Livermore, California 94550

Sandia is a multiprogram laboratory operated by Sandia Corporation,
a Lockheed Martin Company, for the United States Department of
Energy under Contract DE-AC04-94AL85000.

Approved for public release; further dissemination unlimited.



Sandia National Laboratories

Issued by Sandia National Laboratories, operated for the United States Department of Energy by Sandia Corporation.

NOTICE: This report was prepared as an account of work sponsored by an agency of the United States Government. Neither the United States Government, nor any agency thereof, nor any of their employees, nor any of their contractors, subcontractors, or their employees, make any warranty, express or implied, or assume any legal liability or responsibility for the accuracy, completeness, or usefulness of any information, apparatus, product, or process disclosed, or represent that its use would not infringe privately owned rights. Reference herein to any specific commercial product, process, or service by trade name, trademark, manufacturer, or otherwise, does not necessarily constitute or imply its endorsement, recommendation, or favoring by the United States Government, any agency thereof, or any of their contractors or subcontractors. The views and opinions expressed herein do not necessarily state or reflect those of the United States Government, any agency thereof, or any of their contractors.

Printed in the United States of America. This report has been reproduced directly from the best available copy.

Available to DOE and DOE contractors from
U.S. Department of Energy
Office of Scientific and Technical Information
P.O. Box 62
Oak Ridge, TN 37831

Telephone: (865)576-8401
Facsimile: (865)576-5728
E-Mail: reports@adonis.osti.gov
Online ordering: <http://www.doe.gov/bridge>

Available to the public from
U.S. Department of Commerce
National Technical Information Service
5285 Port Royal Rd
Springfield, VA 22161

Telephone: (800)553-6847
Facsimile: (703)605-6900
E-Mail: orders@ntis.fedworld.gov
Online order: <http://www.ntis.gov/ordering.htm>



SAND2001-8184
Unlimited Release
Printed June 2001

The Tritium Performance of Alloy 22-13-5

S. L. Robinson
Gas Transfer Systems and Microsystems Engineering

Sandia National Laboratories
P. O. Box 969
Livermore, CA 94551

Abstract

Previously published studies of the performance of high strength austenitic steels and superalloys in tritium have demonstrated significant shortcomings in toughness and sensitivity to decay helium in the metal matrix. The alloy 22Cr-13Ni-5Mn exhibits high cracking thresholds in hydrogen, and promising performance in tritium-charged and aged smooth tensile specimens. It is readily forged to strengths beyond 690 MPa, and is commercially available. The tensile performance of 22-13-5 is compared to that of 21-6-9 and JBK-75. Aspects of a development program are outlined.

Contents

Abstract	3
Acknowledgments	6
Introduction	7
Hydrogen Isotope Compatibility of 22-13-5	9
Hydrogen compatibility	9
Tritium compatibility	10
Comparison of HERF 22-13-5, HERF 21-6-9 and HERF 304L	19
Elements of a Development Program	24
Forging practice	24
Welding practice	24
Tritium effects on toughness/cracking thresholds	25
Failure Assessment Diagram	25
Demonstration hardware/life storage	25
Conclusions	25
References	27

Figures

Figure 1. The yield and ultimate tensile strengths increase monotonically with helium accumulation. Both yield and ultimate are computed as load/initial area.	13
Figure 2. The uniform strain and strain to fracture decrease with helium accumulation. Both strains are computed from extensometry of the gage length.	14
Figure 3. Low magnification image of fracture surface of specimen tested at 1486 atomic ppm helium-3 and 3974 atomic ppm of tritium. A mixed mode of flat facets and ductile rupture by void growth and coalescence is observed.	15
Figure 4. At higher magnification, the mixed ductile and flat fracture modes are more visible. Distinct ridges of ductile fracture are observed separating the flat facets, leading to the conclusion that the facet formation preceded the void growth and coalescence. The final separation by shear is visible at the bottom of the image.	16
Figure 5. At high magnification, precipitate particles are observed at the bottom of many of the voids. Some secondary cracking is observed normal to the main fracture surface.	17
Figure 6. The flat facets exhibit the intersection line features previously identified ^{2,6} as the intersection of deformation twin bands with grain boundaries. Some precipitate particles are observed on the flat facets, although they do not appear to influence the fracture mode of the grain boundary.	18
Figure 7. The hardening interval between yield and ultimate tensile strength shows that HERF 22-13-5 exhibits a greater work-hardening capability with increasing helium than do HERF 304L and HERF 21-6-9.	20

Figure 8. The strain beyond uniform strain decreases similarly with helium accumulation for the alloys shown, however HERF 22-13-5 exhibits substantially greater strain beyond uniform strain than the other alloys.	21
Figure 9. Both HERF 22-13-5 and HERF 304L exhibit little dependence of the instability stress (true stress at uniform strain) on helium concentration, however 21-6-9 exhibits a decreasing instability stress.	22

Tables

Table I. Nominal compositions of Nitronics [®] 50, Nitronics [®] 40 and JBK-75 in wt. % ...	8
Table II. Target strengths of Nitronics [®] 50, Nitronics [®] 40 and JBK-75.	8
Table III. Helium analyses by vacuum fusion analysis ¹⁰	11
Table IV. Summary of tensile test data for HERF 22-13-5.	12

Acknowledgments

Thanks to Brian Somerday, Neville Moody and Ben Odegard for their encouragement, thought provoking discussions, and reviews of this manuscript. Thanks also to Bert Brown for performing the tensile tests and other necessary tasks in the tritium facility at SNL/CA.

The Tritium Performance of Alloy 22-13-5

Introduction

The Nuclear Weapons Complex continues to need a tritium compatible high-strength alloy, since previously studied high strength alloys, JBK-75 and Nitronics® 40, have exhibited shortcomings. The typical chemistries and target strength values for these alloys, (Nitronics® 40 is also known as 21-6-9), are shown in Tables I and II. Early work with the precipitation strengthened iron base superalloy JBK-75 (a modified A-286) suggested some loss of cracking resistance (K_{th}) in simulated (having microstructure and strength similarities) welds when tested in high pressure hydrogen¹. Tensile tests of weld-like solution-treated and aged microstructures in tritium also exhibited severe losses in tensile properties when high hydrogen concentrations and helium concentrations were present in the metal². In addition, electron beam welds with lack of penetration defects exhibited crack extension in tritium³ and pinch welds cracked in similar environments³. The cracking susceptibility was found to result from a combination of undesirable microstructural elements, high gas inventories within the metal, and high residual stresses which are likely to accompany work-hardenable high strength materials. Indeed, under reduced tritium pressure conditions, crack extension was not observed even after extensive aging³. The precise conditions (environmental and metallurgical) required to induced cracking have not been conclusively identified.

Table I. Nominal compositions of Nitronics® 50, Nitronics® 40 and JBK-75 in wt. %.

Alloy	C	Cr	Ni	Mn	Mo	N	Nb	V	B	Si
N50	0.06	20.5- 23.5	11.5- 13.5	4.0- 6.0	1.5- 3.0	0.2- 0.4	0.1- 0.3	0.1- 0.3	—	1.0
N40*	0.02- 0.04	19.0- 21.5	5.5- 7.5	8.0- 10.0	—	0.2- 0.4	—	—	—	0.3- 0.7
JBK-75#	0.01- 0.03	13.5- 16	29- 31	0.2 max	1.0- 1.5	0.01 max	—	0.1- 0.5	0.002 -max	0.01 max

*Specification 9855212.

#Specification P14462

Table II. Target strengths of Nitronics® 50, Nitronics® 40 and JBK-75.

Alloy	Yield strength, MPa/KSI	Ultimate Strength, MPa/KSI
N50 HERF*	750*/110	1138/165
N40 HERF* ¹	620**/90	862/125
JBK-75 HERF	725#/105	1005/146

*The yield strength is strongly sensitive to thermomechanical treatment and may range from 750 to in excess of 1000 MPa. The reported value is for high energy rate forged N50TM discussed in the text.

**N40 is also sensitive to thermomechanical treatment but does not attain the strengths possible with N50.

Dual age condition 980°C/1Hr/WQ+720°C/16Hr/AC. May also be used in forged condition for more strength.

The Nitronics®40 alloy (21-6-9) offers almost as high a strength as JBK-75, has moderate hydrogen compatibility^{1,4}, and has seen extensive use as a tritium containment material. Subcritical cracking in 21-6-9 is highly sensitive to processing⁵, especially reclamation welding⁵. It exhibits lower tritium exposure limits in pinch welds than forged 304L⁵, and exhibits severe losses in both tensile properties⁶ and cracking resistance⁷ upon long-term aging in tritium.

Recently, an elastic-plastic “safe” operating regime for tritium-aged containment materials, based on the CEGB’s R-6 FAD or Failure Assessment Diagram, has been defined⁸. It has been proposed to incorporate the FAD into DG10215, the Reservoir Design Standard⁹, to assure that

¹ The abbreviations N40 and N50 are used for Nitronics® 40 and Nitronics® 50 respectively.

reservoirs are defect-tolerant. By defect-tolerant, we mean that any defect up to the size detectable at the threshold of NDT inspection will not exhibit crack extension during the lifetime of the containment structure. This is significant since crack propagation rates are not yet predictable, and therefore crack extension must be prevented. As proposed for application within DG10215, significant safety factors are incorporated to protect against such unknown factors as high residual stresses, uncertainties in the stress analysis, material property variation such as strength variations and uncertainties in the conservative measurement of threshold stress intensity for cracking (internal as well as external H-isotope), and variations in NDT sensitivity. Safeguarding against high residual stresses is very important with high strength materials, since high strength implies the capacity for high residual stress. From the FAD⁸ for HERF 21-6-9 it may be demonstrated that the safety factors against crack initiation for 21-6-9 are small for many practical operating conditions, and sensitive to metal working processes. Thus 21-6-9 exhibits inherent drawbacks from the perspective of assuring integrity.

The Nitronics[®] 50 alloy, also known as 22-13-5 (22 Cr-13 Ni-5 Mn bal Fe) offers the potential for a substantial improvement in tritium compatibility in a high strength austenitic alloy. In the following, we review the existing hydrogen embrittlement data, and present previously unpublished tritium effects data on this alloy. We compare the tritium smooth bar tensile properties of 22-13-5 and 21-6-9. This data will demonstrate the above mentioned potential improvements in compatibility. Furthermore, it will support the desirability of a development program including an extended test and qualification program in tritium. The elements of that program are elaborated. The final step of this qualification program is the placement of demonstration hardware into life storage at Westinghouse Savannah River Company.

Hydrogen Isotope Compatibility of 22-13-5

Hydrogen compatibility

Odegard and West¹⁰ examined the tensile behavior of 22-13-5 in warm-worked, high energy rate forged (HERF) and annealed microstructural conditions. Specimens were tested uncharged, in 69 MPa hydrogen, precharged with hydrogen and tested in air, and precharged and tested in 69 MPa hydrogen. Their precharging condition, 200°C in 24.1 MPa hydrogen for 10.5 days,

produced a surface concentration of about 2500 atomic ppm hydrogen, and a gradient within the 3 mm diameter specimen such that the centerline concentration was estimated at 50% of the surface concentration. They observed no degradation in ductility (measured as % reduction of area) or change in fracture mode, and only a small decrease in uniform elongation in these tests, in spite of yield strengths as high as 1240 MPa and nitrogen content to 0.34 %. Slight increases in yield strength were observed in the precharged cases, attributed to hydrogen atmosphere locking of dislocations. Brooks and West¹¹ examined the tensile test behavior of 22-13-5 welds in hydrogen and found them also resistant to hydrogen embrittlement.

Perra¹ measured cracking thresholds in a number of high strength austenitic steels including 21-6-9 and 22-13-5. Measurements were performed on precracked, bolt-loaded WOL specimens at 100 and 200 MPa hydrogen pressure over a period of 5000 hours, at room temperature. Deep side-grooving (25 to 50%) was used to maximize constraint. Although plane strain conditions were not obtained (requiring thickness $B > 2.5(K_{th}/\sigma_y)^2$), the specimen thickness of 22.2 mm was the same as that of other specimens of 21-6-9, JBK-75, etc. No cracking was observed at $145 \text{ MPa}\sqrt{\text{m}}$ in 200 MPa hydrogen in the 22-13-5 at a yield strength of 717 MPa, while a threshold of $109 \text{ MPa}\sqrt{\text{m}}$ was observed in 21-6-9 at a yield strength of 827 MPa. Thus the hydrogen cracking threshold of 22-13-5 appears to be at least 30% greater than that of 21-6-9. It is not known what the effect of yield strength on threshold would be at the higher yield strength of the 21-6-9 tested. Since plane strain conditions were not obtained, this comparison is relevant only to the thicknesses tested.

Tritium compatibility

Tritium charging of 3 mm diameter smooth tensile bars was performed at Sandia in March of 1983. Specimens of high energy rate forged (HERF) 22-13-5 were gas-phase charged at 300°C to a uniform concentration of 5460 atomic ppm, more than twice that at the surface of Odegard and West's⁹ tensile specimens. Specimens were stored in a freezer at -40°C for various time intervals, removed, warmed to room temperature, and tensile tested in air at a strain rate of $3.3 \times 10^{-5} \text{ s}^{-1}$. Further procedural details are available in Robinson and Thomas⁶. The slow testing rate is intended to allow hydrogen embrittlement effects to be more evident. Test times varied from 30 minutes to about 50 minutes depending upon the strain to fracture. While tritium losses

during the test were small and superficial the results may be sensitive to the lack of a hydrogen overpressure¹².

At three aging times, the helium concentration in the specimen gage lengths was measured by vacuum fusion analysis performed by Brian Oliver¹³, then located at Rocketdyne, Canoga Park CA. The helium measurements and associated variation of duplicate specimens is shown in Table III. The initial tritium concentration of 5460 atomic ppm was confirmed by back-calculation using the known rate of decay of tritium to helium-3. The reported helium concentrations in Table III are therefore interpolated to the test date from measured concentrations. The variability is small, and the error of the interpolated helium values is estimated at ± 25 atomic ppm. The tritium concentrations were interpolated similarly.

Table III. Helium analyses by vacuum fusion analysis¹⁰.

Date of analysis (charged March 1983)	Helium Concentration, atomic ppm
August 2 1985	810 \pm 5 (duplicate specimens)
July 25 1986	987 \pm 16 (duplicate specimens)
February 1989	1525 \pm 12 (duplicate specimens)

The tensile test results are tabulated in Table IV, and shown graphically in Figures 1 and 2. Figure 1 shows the yield strength and ultimate strength (engineering ultimate, or load/initial area) while figure 2 shows the uniform strain and strain to fracture, both as a function of helium-3 concentration. The yield and ultimate tensile strength increase slowly with helium concentration, and the work-hardening interval between them decreases with helium concentration. Both uniform and fracture strains decrease with helium concentration, although even at 1426 appm helium and 3036 atomic ppm tritium they remain relatively high. In general, the interval between uniform and fracture strain decreases slowly with helium accumulation.

Table IV. Summary of tensile test data for HERF 22-13-5.

C, He appm	Yield Strength MPa/PSI	Ultimate Tensile Strength MPa/PSI	ϵ_u / ϵ_u , uniform strain	c_f/ϵ_f fracture strain	%RA reduction of area	Instability Stress (true stress at UTS)	
35	764 110,750	950 137,830	0.195 0.178	0.28 0.247	NM	1135 164,575	
370	842 122,140	988 143,260	0.138 0.129	0.25 0.223	NM	1124 163,040	
441	771 111,790	939 136,140	0.15 0.14	0.278 0.245	NM	1080 156,580	
610	867 125,700	1006 145,915	0.1895 0.174	0.30 0.26	NM	1197 173,510	
1075	902 130,835	1028 149,050	0.156 0.145	0.20 0.183	38.3	1188 172,310	
1314	904 131,040	1002 145,250	0.125 0.118	0.1838 0.1687	NM	1127 163,405	
1486	982 142,400	1031 149,515	0.089 0.0853	0.136 0.1275	46	1123 162,800	

NM: Not measured

Fractography was performed using a JEOL 840 scanning electron microscope. We present only the extreme concentration results as an indication of the performance of the alloy at high helium concentration. Figures 3 through 6 portray the fracture surface at increasing magnification. Flat facets with intersecting striations are observed, as previously seen in other tritium-embrittled austenitic alloys. Neither plateau etching nor thin foil TEM examination were performed on this alloy. Nevertheless, we expect the grain boundary markings to be the result of the intersection of deformation twin bands with the grain boundary, as observed in all previous TEM studies of tritium-aged austenitic alloys^{2,5}. Several areas of flat fracture are observed in Figure 4 which do not exhibit triple points, and thus may represent a transgranular fracture process such as twin plane parting. Substantial amounts of ductile rupture, initiating at fine chromium and vanadium carbonitrides, are observed next to the flat grain facet fractures.

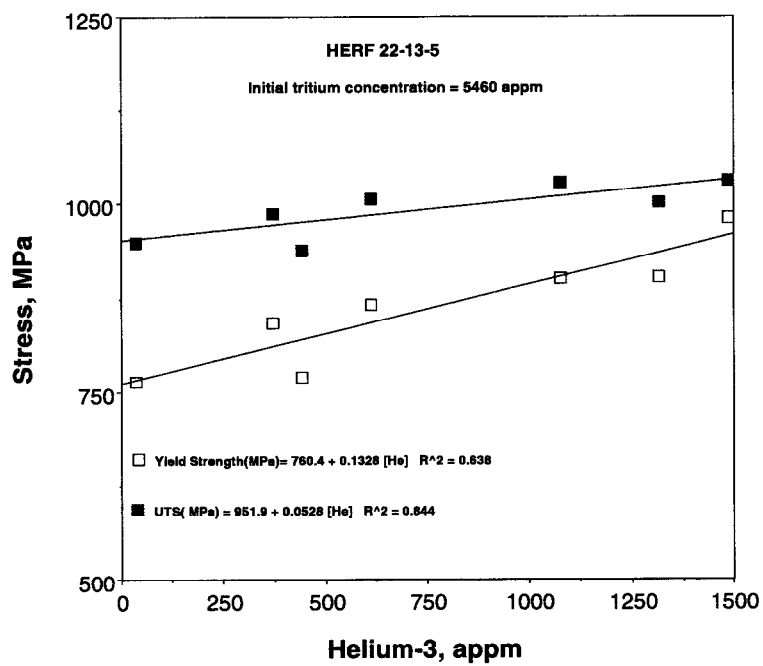


Figure 1. The yield and ultimate tensile strengths increase monotonically with helium accumulation. Both yield and ultimate are computed as load/initial area.

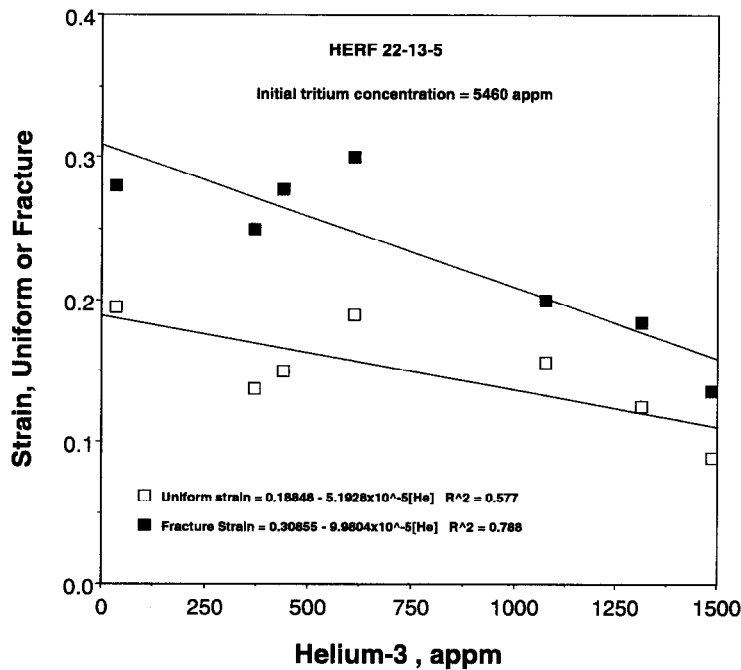


Figure 2. The uniform strain and strain to fracture decrease with helium accumulation. Both strains are computed from extensometry of the gage length.

There are several possible interpretations of these observations of extensive post-ultimate tensile strength strain and ductile rupture. Normal void nucleation, growth and coalescence at carbonitride particles may dominate the post-ultimate tensile strength regime, reducing the amount of grain facet fracture, or blunting the facets and reducing their propagation. Additionally, the early nucleation of voids at carbonitrides would redistribute the stress, slowing the formation of the twinning-induced grain facets. Yet another possibility is that the carbonitride interfaces trap helium, preventing much of it from precipitating on dislocations, and preserving dislocation-controlled deformation at high total helium concentrations. The retention of dislocation-controlled flow instead of twinning-dominated flow at high helium concentrations is an important source of resistance to the combined effects of tritium and helium^{2,5}. Clearly, more detailed study is required to clarify the mechanisms by which 22-13-5 is able to resist severe embrittlement at high helium concentrations.

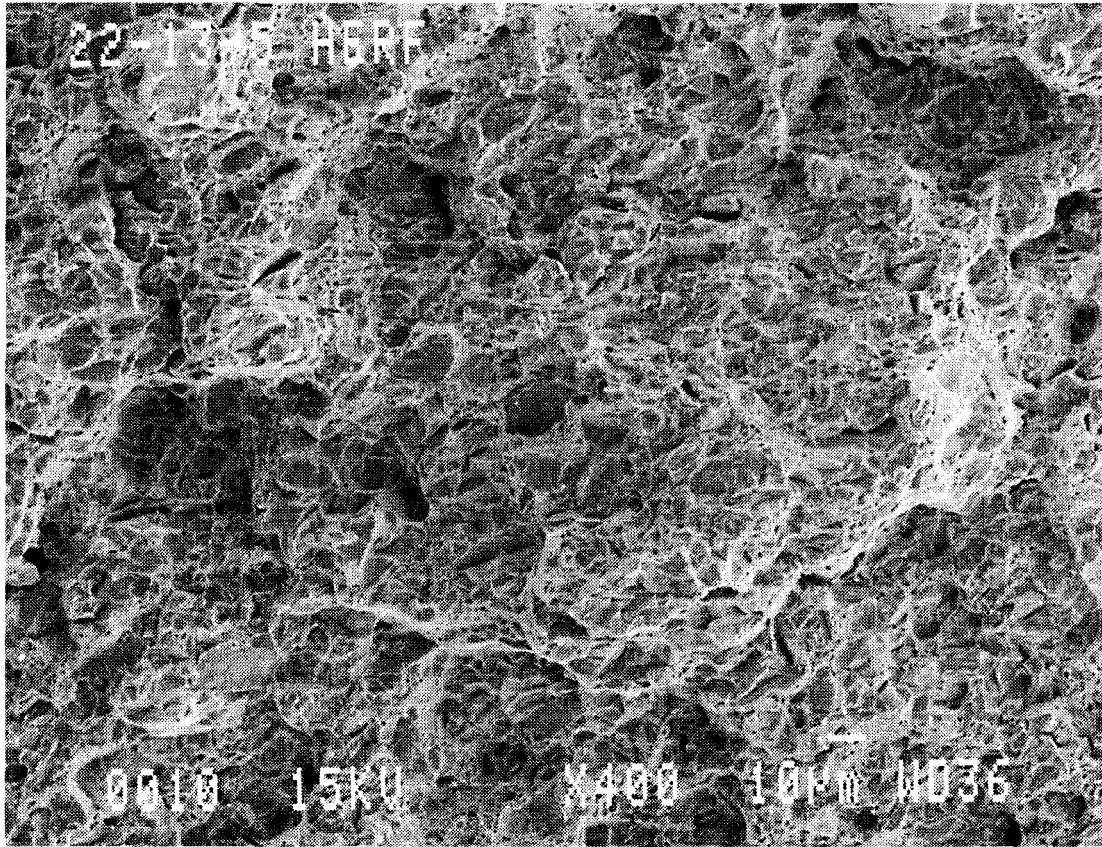


Figure 3. Low magnification image of fracture surface of specimen tested at 1486 atomic ppm helium-3 and 3974 atomic ppm of tritium. A mixed mode of flat facets and ductile rupture by void growth and coalescence is observed.

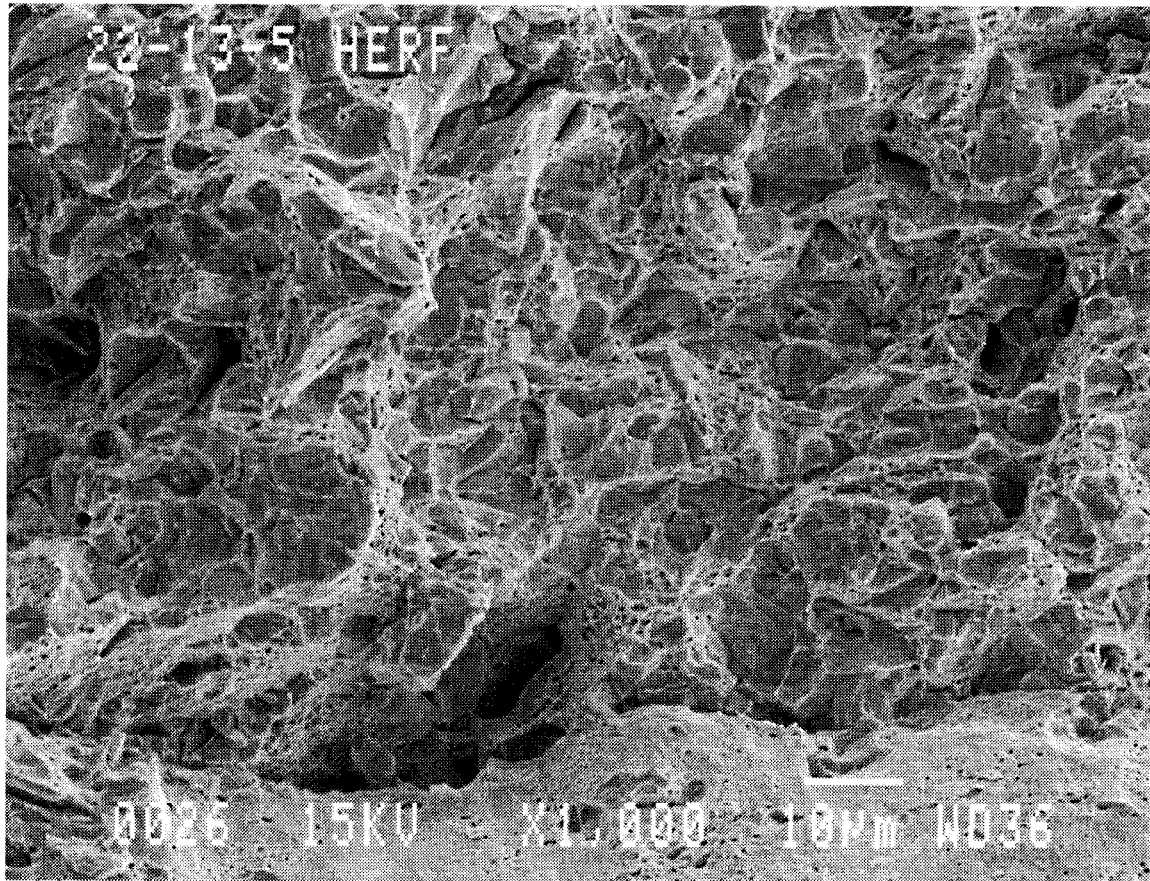


Figure 4. At higher magnification, the mixed ductile and flat fracture modes are more visible. Distinct ridges of ductile fracture are observed separating the flat facets, leading to the conclusion that the facet formation preceded the void growth and coalescence. The final separation by shear is visible at the bottom of the image.

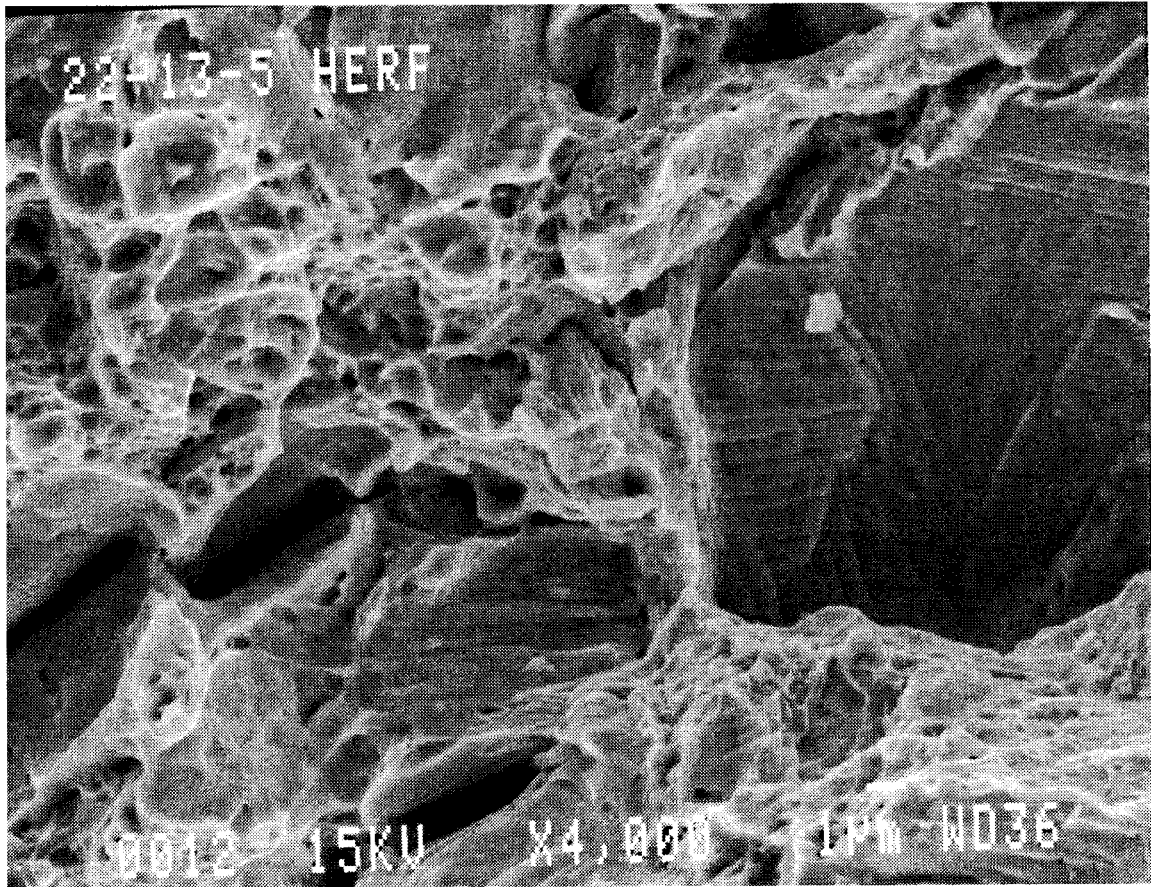


Figure 5. At high magnification, precipitate particles are observed at the bottom of many of the voids. Some secondary cracking is observed normal to the main fracture surface.

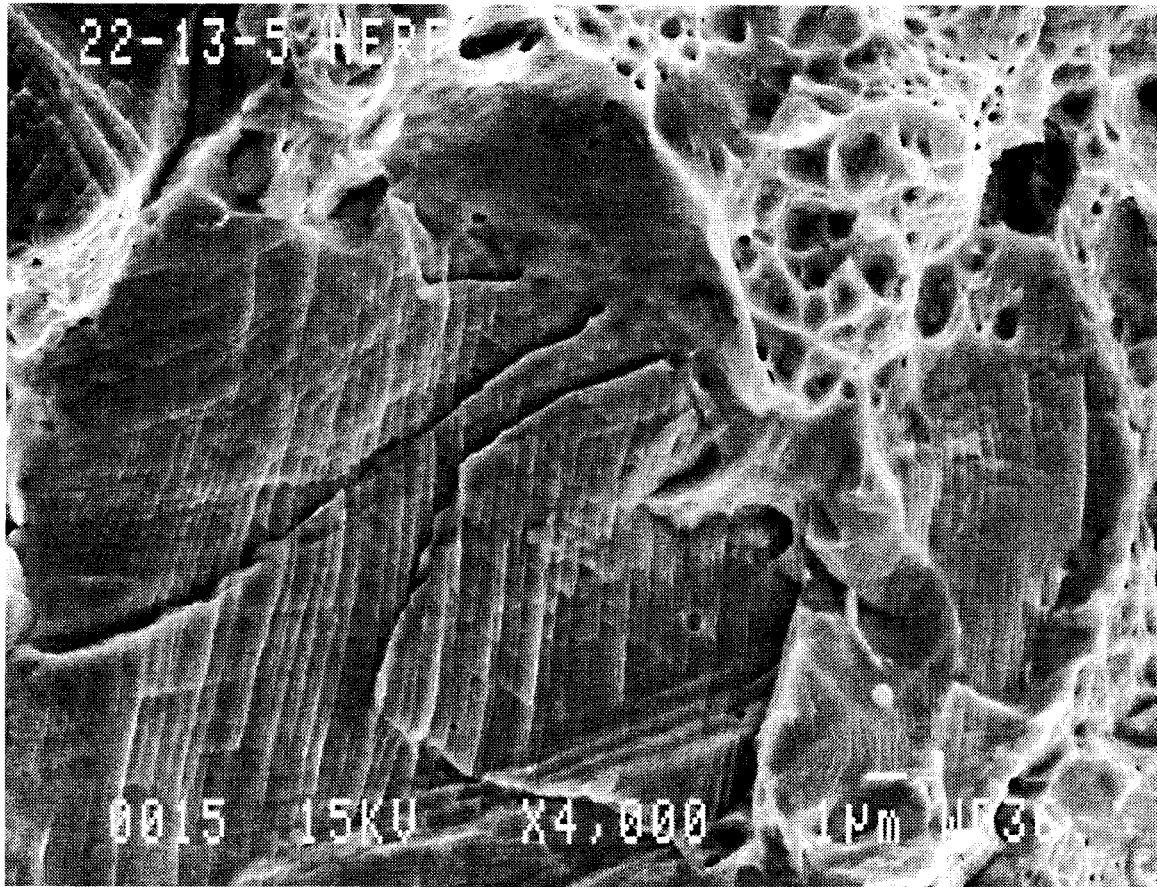


Figure 6. The flat facets exhibit the intersection line features previously identified^{2,6} as the intersection of deformation twin bands with grain boundaries. Some precipitate particles are observed on the flat facets, although they do not appear to influence the fracture mode of the grain boundary.

Comparison of HERF 22-13-5, HERF 21-6-9 and HERF 304L

We may compare the tensile specimen tritium/helium performance of HERF 22-13-5, 21-6-9 and 304L under equivalent tritium charging conditions, since the specimens were charged together. However, the levels of dissolved tritium vary. From these studies, the 22-13-5 appears to dissolve 10- 20% more tritium than does 21-6-9, which in turn dissolves about 170% more than 304L. Nevertheless, on a per unit helium basis, it appears to be more tolerant of tritium and helium than 21-6-9 and 304L.

Figure 7 shows the rates of loss in hardening between yield and true ultimate tensile strength. The absolute amount of hardening of 22-13-5 is about twice that of 21-6-9 and the rate of decrease with helium concentration is somewhat slower. This observation suggests that in 22-13-5 there is relatively more dislocation activity, probably in the form of cross-slip, as opposed to deformation twinning, than in 21-6-9, which may contribute to the greater compatibility. Alternatively, the higher stacking fault energy may give greater cross-slip, increasing the rate of hardening. Figure 8 shows the loss in strain between the uniform strain (at the ultimate strength) and the fracture strain for the alloys. The retention of dislocation-controlled flow instead of twinning-dominated flow at high helium concentrations is an important source of resistance to the combined effects of tritium and helium.^{2,5}

Detailed fractography by “plateau etching” of 21-6-9 found only a few cracked grain facets below the final fracture surface. Those facets exhibited extensive ductility at the ends of the grain facets, but always terminated at grain triple points. This study has not been performed for 22-13-5, and would aid in understanding the roles of void nucleation and relative amounts of dislocation activity between 22-13-5 and 21-6-9.

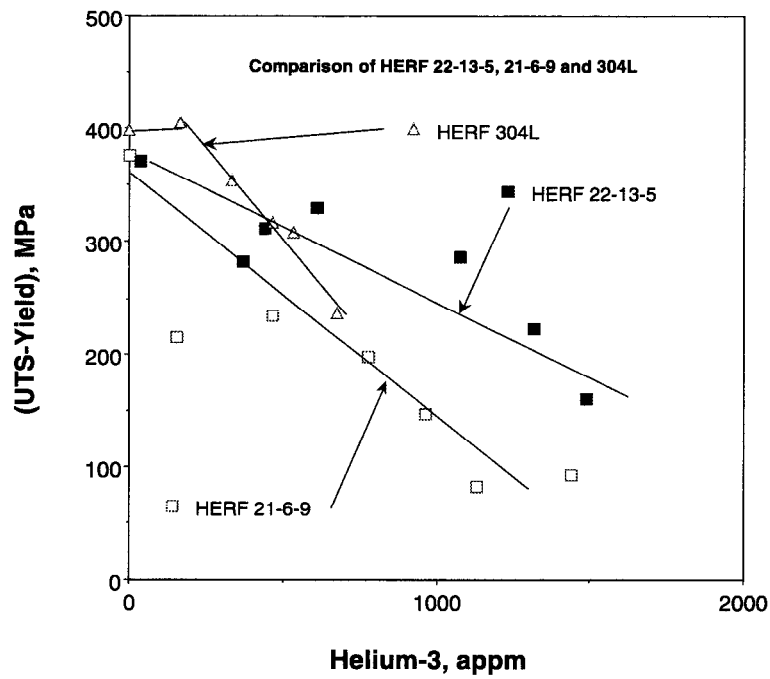


Figure 7. The hardening interval between yield and ultimate tensile strength shows that HERF 22-13-5 exhibits a greater work-hardening capability with increasing helium than do HERF 304L and HERF 21-6-9.

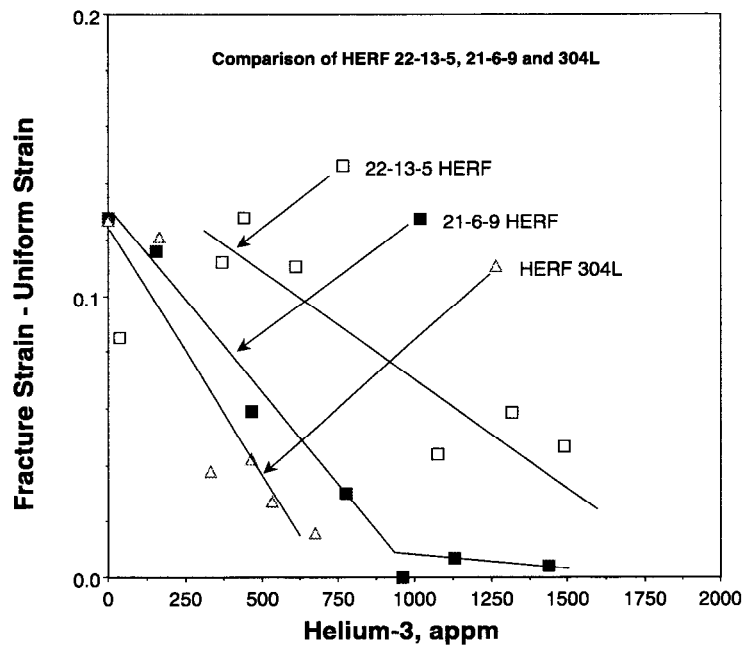


Figure 8. The strain beyond uniform strain decreases similarly with helium accumulation for the alloys shown, however HERF 22-13-5 exhibits substantially greater strain beyond uniform strain than the other alloys.

Finally, Figure 9 shows the true stress at ultimate, the instability stress, for all three materials. (Figure 1 showed the ultimate tensile strength, the “engineering UTS”, as load/initial area.) HERF 304L and 22-13-5 display almost no dependence upon the helium concentration, although a random 10% variability appears to exist. HERF 21-6-9 shows instead a continuous decrease in the instability stress. This is a puzzling observation, and cannot be understood without clarifying the roles of the work-hardening mechanism (twinning vs. dislocation nucleation and intersection), and mechanisms of void growth (grain facet cracking and ductile rupture at carbonitrides).

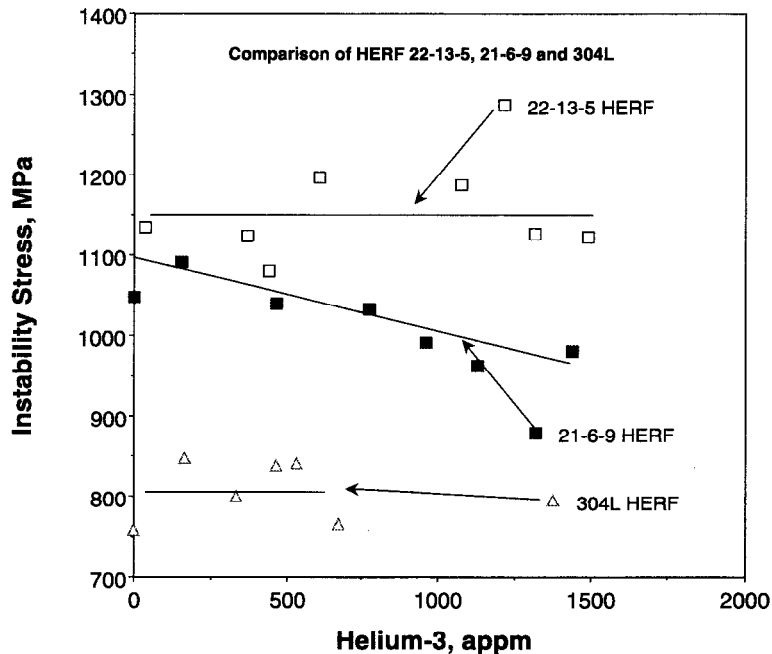


Figure 9. Both HERF 22-13-5 and HERF 304L exhibit little dependence of the instability stress (true stress at uniform strain) on helium concentration, however 21-6-9 exhibits a decreasing instability stress.

A primary engineering concern is for the lifetime of a tritium pressure vessel, which will depend upon how severely and rapidly the tensile properties degrade with tritium exposure. Lifetime is somewhat dependent upon how much tritium an alloy dissolves. At equivalent pressure, 22-13-5 will accumulate 1500 atomic ppm of helium in the time required for 21-6-9 to accumulate 1240 atomic ppm and 304L to accumulate 610 atomic ppm. A high strength alloy will tend to be used at a higher pressure, further increasing the gas load and aging rate. We will use the yield strength for comparison of the gas concentration when the steels are used at maximum allowable pressure, since the pressure capability is proportional to the yield strength⁸.

Assuming ideal gas behavior (Sievert's law) solely for comparison purposes, the relative rates of aging are proportional to the square root of yield strength. Accordingly, in comparing 21-6-9 to

22-13-5, the helium concentration in figures 7-9 applicable to 22-13-5 should be increased by $(750/620)^{1/2} = 1.10$ and the fracture strain at the higher helium value should be used for comparison with 21-6-9. With this factor in mind, we see from Figures 7-9 that 22-13-5 retains a substantial advantage in its tensile performance in tritium.

Published models relating tensile behavior with toughness may be used to estimate and compare cracking resistances. While these comparisons are not quantitative, they may be instructive as to general trends. The tritium cracking resistance of JBK-75 was successfully correlated¹⁴ with tensile data and microstructure using a critical strain model by Lee, Majno and Asaro¹⁵. The threshold fracture toughness K_{TH} is related to the fracture strain through the relation

$$K_{TH} = 6\sqrt{\sigma_0 E L^* \epsilon_f} \quad (1)$$

in which σ_0 is the flow stress (the average of yield and ultimate strength), E is the elastic modulus, L^* is the critical microstructural feature, and ϵ_f is the crack tip plane strain fracture strain. We assume that (1) applies to the intergranular fracture case, and for comparison purposes ignore the fact that the prefactor may change due to constraint. Since the grain facet fracture is similar for all alloys, this assumption is reasonable. Smooth bar fracture strain is corrected to plane strain ductility at the crack tip by substituting¹⁴ $\epsilon_{SMOOTH}/12$ for ϵ_f . Comparison of 21-6-9 and 22-13-5 then suggests that for equivalently tritium charged specimens, the toughness (cracking threshold) of 22-13-5 may be as much as twice that of 21-6-9 provided L^* is similar for the two steels. This assumption is reasonable since L^* appears to be related to the grain size. Only experimental observation can confirm this suggestion; however the comparison provides strong reasons for performing the work.

The sources of excess tritium solubility, the formation of potentially beneficial tritium trapping sites, and the dispersal of helium to apparently non-damaging microstructural elements need to be examined, in order to understand the sources of the compatibility of 22-13-5. Thermal desorption spectroscopy (TDS) may play a significant role in this study. These factors, helium trapping and dispersal may be useful in optimization of the properties. An improved understanding of twinning susceptibility and the role of helium bubble pinning would improve our understanding of methods of optimizing tritium resistance. The results presented here are for

one alloy heat. The study of several heats of the alloy, having different compositions, grain structures and precipitate distributions, should support this activity and those discussed below.

Elements of a Development Program

Forging practice

Forging practice for 22-13-5 is expected to differ from that of 21-6-9 and 304L, particularly with regard to the forging temperatures and work imparted at each stage. Nevertheless, the goals are the same: (1) to produce a moderate dislocation density throughout the shape, (2) to control grain size to a moderate size of ca. ASTM 5, and (3) to exercise control over the flow lines. The dislocation density imparts somewhat elevated, uniform strength and reduces the tritium susceptibility. Control of grain size ensures that multiple grain boundaries exist within a part, and that no single large grain boundary is unfavorably oriented. Flow line control is necessary to ensure that preferential diffusion paths to external surfaces do not exist. As in the past, some development forgings manufactured on forge shop equipment will be necessary. It is possible that press forming will produce the desired properties and that Dynapac® HERF hammers will not be required. Recently (1996) Mataya et al¹⁶ have studied the hot working characteristics of 22-13-5, so current expertise is available for assistance in forging development. Significant differences in metalworking from 304L and 21-6-9 practice may be expected; the carbonitride precipitates control recrystallization and grain growth, and apparently contribute a propensity toward shear localization¹⁵. This tendency can be controlled through careful forging practice. Avoiding the formation of brittle phases¹⁶ will also require careful processing.

Welding practice

The mechanical properties of fusion welds (GTA, electron beam, laser) in 22-13-5 have been studied but not extensively. Welding development work is needed to understand the metallurgy of the welding process. Similarly, solid state welds such as pinch welds, plug welds and resistance forge welded main structural welds have not been studied. We need to prioritize this list of possible processes; the primary joining processes of GTA and Electron Beam welding will be investigated first. A primary issue in electron beam welding will be retaining manganese and nitrogen; the high vapor pressures of these elements predispose the weldments toward loss of

these constituents accompanied by the production of defects. The presence of particulate in the fusion zone may also present problems of vaporization under the beam.

Although it is not planned to reclaim vessels in the future, having a viable process and adequate aging data to allow reclamation would protect against interruptions of supplies in new hardware.

Tritium effects on toughness/cracking thresholds

Although the hydrogen cracking properties look favorable, and the tritium-charged smooth bar tensile properties are encouraging, the final test of viability is the resistance of as-forged microstructures and welded structures to cracking from the combined tritium and helium build-in effects. A variety of compositions, thermomechanical preparations, and welds will require testing in tritium.

Failure Assessment Diagram

As noted in the introduction, a common failing of both 21-6-9 and JBK-75 is their loss in slow crack growth resistance from tritium exposure. Data from the tritium effects program would allow construction of an appropriate failure analysis diagram, quantifying the available design space in terms of both weld and base metal properties. Improvements over the previous high strength alloys would permit the use of adequate safety factors.

Demonstration hardware/life storage

The final step of the process is the successful storage of demonstration hardware, exposed at extreme conditions, to demonstrate the robustness of the material to the extremes of possible service environments. The introduction of hardware into storage may precede the previous two steps.

Conclusions

The high strength steel alloys that have been previously studied for hydrogen and tritium containment have exhibited shortcomings in their process sensitivity and in their tritium aging sensitivity. Therefore, a need persists for a high strength hydrogen- and tritium-compatible material. The hydrogen compatibility of the 22-13-5 alloy was initially

characterized in the '70's and early '80's, and some work on the thermomechanical treatment of the alloy has been performed. That work indicates that 22-13-5 offers a substantially greater amount of hydrogen compatibility than 21-6-9 at no loss in useable strength. Previously unpublished tritium compatibility data indicates that tritium pre-charged and aged 22-13-5 exhibits substantial tritium compatibility as assessed by smooth bar tensile tests. Theoretical fracture models suggest that significant improvements may be obtained in the threshold stress intensity value as tritium aging occurs. Therefore, an effort should be made to develop 22-13-5 for those applications where a high strength hydrogen isotope containment alloy is needed. A development program addressing thermomechanical treatment, weldments and cracking resistance in tritium is proposed, culminating in the storage of demonstration hardware.

References

- ¹ M.W. Perra, "Sustained Load Cracking of Austenitic Steels In Gaseous Hydrogen", Pp. 321-333, in Environmental Degradation of Engineering Materials In Hydrogen, Proceedings of the 2nd International Conference on Environmental Degradation of Engineering Materials, Sept. 21-23, 1981, Virginia Polytechnic Institute, Blacksburg VA 2406, VA Tech Printing Dep't.
- ² S.L. Robinson and N.Y.C. Yang, "The Origins of Tritium and Helium Effects On The Tensile Properties of Metals", Proceedings of The Fourth Topical Conference on Tritium Technology, September 29-October 4, 1991, Albuquerque New Mexico, Fusion Technology 21, no. 2 part 2, (1992), 856
- ³ C.A. Angerman, "Life Storage Testing of Tritium Reservoirs (U), Volume V-JBK-75 Reservoirs", WSRC-RP-91-46-Vol. 5, Secret, RS8232-2/9205825, May 7, 1992.
- ⁴ B.C. Odegard, J.A. Brooks, and A.J. West: in *Effect of Hydrogen of Behavior of Metals*, A.W. Thompson and I.M. Bernstein, eds., AIME, New York, NY, 1976, pp. 116-128.
- ⁵ C.A. Angerman, "Life Storage Testing of Tritium Reservoirs [U], Volume IV-21-6-9 Reservoirs, WSRC-RP-91-46-Vol. 4, Secret, RS8232-2/920497, May 6, 1992.
- ⁶ S.L. Robinson, G.J. Thomas, "Accelerated Fracture Due To Tritium and Helium In 21-6-9 Stainless Steel", Metallurgical Transactions A, 22A, (1991)879-886.
- ⁷ M.J. Morgan, "Tritium and Decay Helium Effects on Cracking Thresholds and Velocities in Stainless Steel" (U), WSRC-MS-99-00343.
- ⁸ S.L. Robinson, Y-R. Kan, "Proposed Update to the Reservoir Design Standard", report SAND2000-8227, March 2000, Sandia National Laboratories.
- ⁹ Specification number DG10215-000 Issue A, "WR Reservoir Design Standard [U]", Secret, DG000010215/20012258, cage code 14214, E.A. English and B.L. Davis, Release No. 93015SL-TER.
- ¹⁰ B.C. Odegard, A.J. West, "On the Thermo-Mechanical Behavior and Hydrogen Compatibility of 22-13-5 Stainless Steel", Mater. Sci. Eng. 19, (1975) 261-270.
- ¹¹ J.A. Brooks and A.J. West, 1981, "Hydrogen induced ductility losses in austenitic stainless steel welds", Met. Trans. A, pp. 213-223; J.A. Brooks, A.J. West and A.W. Thompson, 1983, "Effect of weld composition and microstructure on hydrogen assisted fracture of austenitic stainless steels", Met. Trans. A, pp. 73-84.
- ¹² I.M. Bernstein, R. Garber, G.M. Pressouyre, "Effect of Dissolved Hydrogen on Mechanical Behavior of Metals", P. 37-58 in *Effect of Hydrogen on Behavior of Material*, Proceedings of an International Conference, Jackson Lake Lodge Wyo., 1975, Eds. A.W. Thompson and I.M. Bernstein, AIME, 1976.
- ¹³ H. Farrar IV and B.M. Oliver, "A Mass Spectrometer System to Determine Very Low Levels of Helium in Small Solid and Liquid Samples", J. Vac. Sci. Technol. A, 4, (1986) 1741.

¹⁴ S.L. Robinson and N.R. Moody, "The Effect of Hydrogen and Tritium on Crack Growth Resistance in Stainless Steel Superalloys", *Journal of Nuclear Materials* , 140(1986)245-251.

¹⁵ S. Lee, L. Majno and R.J. Asaro, *Metall. Trans. A*, 16A, (1985), 1633-1648.

¹⁶ M.C. Mataya, C.A. Perkins, S.W. Thompson, and D.K. Matlock, "Flow Stress and Microstructural Evolution During Hot Working of Alloy 22Cr-13Ni-5Mn-0.3N Austenitic Stainless Steel", *Metallurgical and Materials Transactions A*, 27A (1996), 1251-1266.

Distribution

- 1 US NNSA
Albuquerque Operations Office
Att'n. J. Claycomb
P.O. Box 5400
Albuquerque, N.M. 87185-5400
- 1 US NNSA
Albuquerque Operations Office
Att'n. E. Whiteman
P.O. Box 5400
Albuquerque, N.M. 87185-5400
- 1 Honeywell Ind.
Kansas City Division
Att'n: R. Hanlin
P.O. Box 41959
Kansas City MO 64141-6159
- 1 University of California
Los Alamos National Laboratories
Att'n: K. Keeler, G780
P.O. Box 1663
Los Alamos, N.M. 87545
- 1 University of California
Los Alamos National Laboratories
Att'n: J. Straw, G780
P.O. Box 1663
Los Alamos, N.M. 87545
- 1 University of California
Los Alamos National Laboratories
Att'n: L. Salazar, NW-SS, F630
P.O. Box 1663
Los Alamos, N.M. 87545
- 1 University of California
Lawrence Livermore National Laboratory
Att'n: Ed Dalder
P.O. Box 808
Livermore, CA 94550

Distribution (Continued)

1	Savannah River Site Att'n: M. Morgan Bldg 773-A Aiken, SC 29801
1	MS-9001 M.E. John, 8000 Att'n.: R.C. Wayne, 2200, MS9005 J. Vitko, 8100, MS9004 W.J. McLean, 8300, MS9054 D.R. Henson, 8400, MS9007 P.N. Smith, 8500, MS9002 K.E. Washington, 8900, MS9003 D.L. Crawford, 9900, MS9003
1	MS-9005 E. Cull, Jr., 2260
1	MS-9108 M. Hardwick, 8414
10	MS-9108 S.L. Robinson, 8414
1	MS-9108 G. Story, 8414
1	MS-9108 R. Ng, 8414
1	MS9402 K. Wilson, 8724
1	MS-9402 N. Moody, 8724
1	MS-9402 J. Brooks, 8724
1	MS-9402 C. Cadden, 8723
1	MS-9402 B. Odegard, Jr., 8724
1	MS-9402 B. Somerday, 8724
1	MS-9403 D. Hughes, 8726
1	MS9405 R.H. Stulen, 8700 Att.: J.M. Hruby, 8702, MS-9401 D.E. Koker, 8709, MS9017 R.Q. Hwang, 8721, MS9161 W.A. Kawahara, 8725, MS9042 E.P. Chen, 8726, MS9042 J.L. Handrock, 8727, MS9042 C.C. Henderson, 8729, MS9401
3	MS-9018 Central Technical Files, 8940-2
1	MS-089 Technical Library, 4916
1	MS-9021 Classification Office, 8511/Technical Library, MS0899, 4916
1	MS-9021 Classification Office, 8511 for DOE/OSTI